Desensitization of mechano-gated K_{2P} channels

Eric Honoré*†, Amanda Jane Patel*, Jean Chemin‡, Thomas Suchyna§, and Frederick Sachs†§

§Single Molecule Biophysics, 301 Cary Hall, University at Buffalo, State University of New York, Buffalo, NY 14214; *Institut de Pharmacologie Moléculaire et Cellulaire, Unité Mixte de Recherche 6097, Centre National de la Recherche Scientifique, 660 Route des Lucioles, 06560 Valbonne, France; and ‡L'Institut de Génétique Humaine, Unité Propre de Recherche 1142, Centre National de la Recherche Scientifique, 141 Rue de la Cardonille, 34396 Montpellier Cedex 5, France

Edited by Ramón Latorre, Center for Scientific Studies, Valdivia, Chile, and approved March 14, 2006 (received for review February 1, 2006)

The neuronal mechano-gated K_{2P} channels TREK-1 and TRAAK show pronounced desensitization within 100 ms of membrane stretch. Desensitization persists in the presence of cytoskeleton disrupting agents, upon patch excision, and when channels are expressed in membrane blebs. Mechanosensitive currents evoked with a variety of complex stimulus protocols were globally fit to a four-state cyclic kinetic model in detailed balance, without the need to introduce adaptation of the stimulus. However, we show that patch stress can be a complex function of time and stimulation history. The kinetic model couples desensitization to activation, so that gentle conditioning stimuli do not cause desensitization. Prestressing the channels with pressure, amphipaths, intracellular acidosis, or the E306A mutation reduces the peak-to-steady-state ratio by changing the preexponential terms of the rate constants, increasing the steady-state current amplitude. The mechanical responsivity can be accounted for by a change of in-plane area of ≈2 nm² between the closed and open conformations. Desensitization and its regulation by chemical messengers is predicted to condition the physiological role of K_{2P} channels.

amphipaths | kinetics | stretch | TRAAK | TREK-1

Most receptors, including ligand-gated ion channels, desensitize with continuous stimulation. Desensitization is a reversible, use-dependent, form of signal plasticity critical for maintaining the dynamic sensitivity over a wide dynamic range. Desensitization also protects cells from inappropriate persistent activation. Many mechano-gated ion channels desensitize (1–5). There are two basic mechanisms that account for desensitization: adaptation and inactivation. Adaptation refers to the uncoupling of the stimulus from the channel, whereas inactivation refers to a block of the permeation path. In hair cells of the inner ear, deflection opens a mechano-gated channel at the tip of the stereocilium leading to depolarization (6). A fast adaptation mechanism (0.3–5 ms) is attributed to the binding of calcium near the channel after permeation through the open ionic pore (6), i.e., Ca^{2+} block. A slower adaptation (10–100 ms) occurs when the calcium-dependent molecular motor myosin-1c, which pulls on the channels, slips down the actin cytoskeleton reducing the force applied to the channel (6).

Rapid desensitization also occurs in mechanosensitive channels expressed in nonspecialized cells. For instance, the stretch-activated cation channel of *Xenopus* oocyte opens transiently in response to a step change in patch pressure (5). The decrease in current has been attributed to relaxation of the mechanical stimulus, although as shown in this work, that interpretation may not be a good discriminator. Desensitization of the oocyte channel is fragile and may disappear when patches are repetitively stimulated (5). This fragility was attributed to decoupling of the bilayer from the cytoskeleton (5).

Stretch-activated K^+ channels are present in neurons of both the central and the peripheral nervous systems (7–9), and they also have been described in nonnervous tissue including the heart and gastrointestinal tract (4, 10–12). In rat atria, the mechanosenstive K^+ currents decline to a plateau of 20–30% of peak within ≈1 s (4). These channels share the functional properties of the TREK/TRAAK K_{2P} channels and show a similar pattern of expression (13–16). The K_{2P} subunits have four transmembrane segments and two P domains in tandem so the functional K_{2P} channel is a dimer (for reviews, see refs. 17 and 18).

TREK-1/-2 and TRAAK are modulated by multiple physical and chemical stimuli (17). Membrane stretch reversibly opens channels, whereas amphipaths may either open or close them (13). TREK-1 is opened by intracellular acidosis in the absence of mechanical stimulation (19). This effect is critically dependent on the negative charge of a glutamate residue at position 306 in the proximal C-terminal domain (20). Titration of E306 at acidic pH, or substitution of this glutamate with an alanine, dramatically increases TREK-1 activity (20). E306 exerts its control through a nearby cluster of positive charges (a PIP_2 interaction domain) that appears to interact with the negatively charged inner leaflet of the bilayer (21).

By using a high-speed pressure servo (22), we demonstrate here that TREK-1 and TRAAK show pronounced desensitization, similar to native stretch-sensitive K^+ channels. Kinetic models show that desensitization can be accounted for without introducing adaptation of the stimulus. We favor a physical model of gating that utilizes torque about some point within the membrane interior (23, 24).

Results

Striking step pulses of pressure evoked nanoampere currents in cell-attached patches of TREK-1 transfected COS cells (Fig. 1*A*). No stretch-sensitive K^+ channels were visible in mock-transfected cells (see Fig. 6*A*, which is published as supporting information on the PNAS web site). Increasing steps of negative pressure elicited progressively larger currents (Fig. 1*A*). The currents rose with a latency of several milliseconds that was nearly independent of the stimulus amplitude, peaked in ≈20 ms, and desensitized over ≈100 ms. The desensitization was monoexponential with a time constant of 46 ± 4.2 ms ($n = 28$) at −50 mmHg (1 mmHg = 133 Pa). Excision to the inside-out configuration greatly increased the amplitude of the currents, but they still desensitized ($\tau = 76 \pm 6.7$ ms at −50 mmHg; $n = 22$; Fig. 1*B*). Fitting the peak currents with a Boltzmann distribution [$I = iN/(1 + e^{k(P-P_{1/2})})$, where i is the unitary current and N is the number of channels], and extrapolating it to saturation gave $N \sim 920$ in this patch (see Fig. 6*D*). For TREK-1 in excised inside-out patches $P_{1/2} = -53.1 \pm 3.5$ mmHg and $k = 10.1 \pm 0.69$ ($n = 20$) (note, for a two-state model with state 1 = closed and state 2 = open, and pressure sensitivities k_{12}^1, k_{21}^1, then $k = k_{12}^1 - k_{21}^1$ and $P_{1/2} = \ln(k_{21}/k_{12})_{P=0}/k$).

Desensitization persisted when cells were treated (in culture) with the actin-disrupting agent latrunculin A ($\tau = 56.9 \pm 11.1$ ms at −50 mmHg; $n = 12$) or the tubulin-disrupting agent nocoda-

Conflict of interest statement: No conflicts declared.

This paper was submitted directly (Track II) to the PNAS office.

Abbreviation: pH_i, intracellular pH.

†To whom correspondence may be addressed. E-mail: honore@ipmc.cnrs.fr or sachs@buffalo.edu.

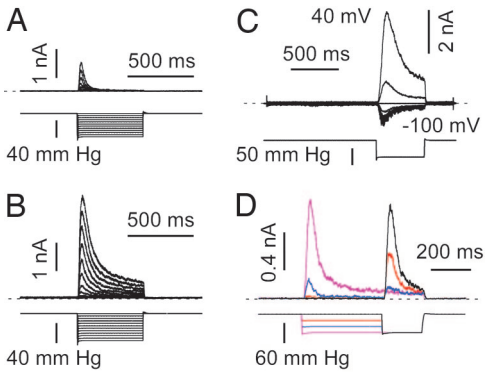

Fig. 1. Desensitization of TREK-1. (*A*) Currents recorded in a cell-attached patch at a holding potential of 0 mV in a physiological K^+ gradient (upper trace). The pressure steps (lower trace) were applied every 5 s. (*B*) Currents from the same patch 5 min after excision to the inside-out mode. (*C*) Desensitization is nearly voltage independent; inside-out patch without internal or external divalent cations and symmetric K^+; holding potential was 0 mV, and the voltage was increased by steps of 20 mV from −100 to 40 mV every 3 s (voltage trace not shown). A negative pressure pulse of −50 mmHg (lower trace) opened the channels at each potential. (*D*) A double pressure-pulse protocol applied to a cell-attached patch; 0 mV pipette potential, physiological K^+ gradient; zero current is indicated by a dashed line. Pressure pulses were applied every 3 s.

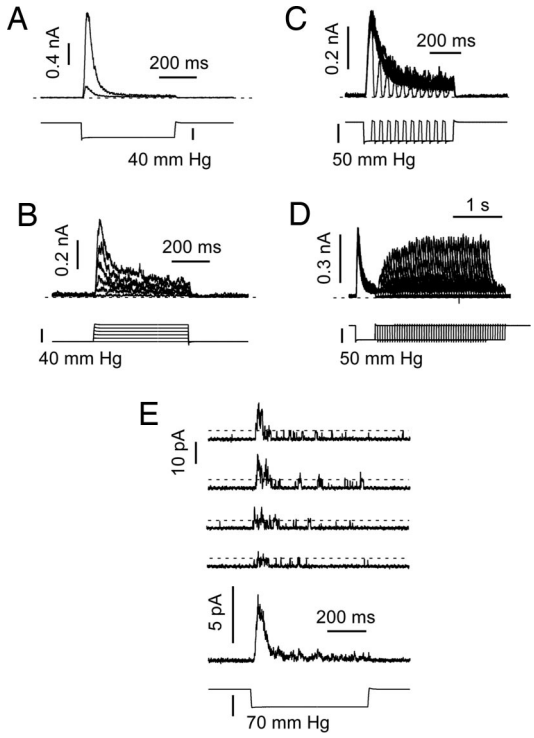

Fig. 2. Desensitization of TRAAK. (*A*) TRAAK current was recorded in the cell-attached mode (smaller current) and then inside-out (larger current). Holding potential was 0 mV in physiological K^+ gradient (upper trace). The pressure pulse (lower trace) was applied every 3 s. (*B*) Pressure response with steps of increasing positive pressure (lower traces). Holding potential was 0 mV in physiological K^+ gradient (upper trace); pulses were delivered every 3 s. (*C*) The rapid turn-off of currents at different times during desensitization. Holding potential was 0 mV, and pressure pulses were every 3 s in physiological K^+ gradient. (*D*) Recovery from inactivation (upper traces) using double pulse protocols with variable delay (lower traces). Pulses were applied every 6 s. In *A–D*, zero current is indicated by a dashed line. (*E*) Single channel currents show desensitization primarily by a reduction in the opening rate and with constant unitary currents. Holding potential was 0 mV with pressure pulses every 3 s in physiological K^+ gradient. The lowest current trace is the average of 20 single channel traces. The amplitude of a single channel current is indicated by the dashed lines.

zole ($\tau = 35.2 \pm 4.1$ ms at −50 mmHg; $n = 10$) (Fig. 6 *B* and *C*). Latrunculin A significantly ($P < 0.01$) increased the amplitude of the current stimulated by pressure, mimicking the effect of patch excision (see ref. 25); at −60 mmHg the control cell-attached current amplitude (in the presence of DMSO) was 365 ± 184 pA; after latrunculin A, 1448 ± 314 pA; after nocodazole, 346 ± 85 pA; and after excision to inside-out, 1751 ± 349 pA ($n = 15$) (see Figs. 1 *A* and *B* and 6 *B* and *C*).

Desensitization occurred in the absence of intracellular and extracellular divalent cations and with inward and outward currents in symmetrical K^+ (Fig. 1*C*). The kinetics were not significantly affected by membrane potential, suggesting that neither activation nor desensitization involved movement of charged groups within the membrane ($\tau = 60.8 \pm 3.8$ ms and $n = 9$; and $\tau = 72.8 \pm 7.7$ ms and $n = 9$, for a pressure pulse of −50 mmHg at −80 and +80 mV, respectively; Fig. 1*C*).

By using double pulse protocols to probe the kinetics of desensitization, a prepulse of negative pressure led to a decrease in the current amplitude to the test pulse (Fig. 1*D*). Note that for an intermediate prepulse pressure of −40 mmHg (blue current trace), the current elicited by a test pulse of −60 mmHg became almost noninactivating (although smaller in amplitude; Fig. 1*D* and see also Fig. 4*C*).

Currents from TRAAK channels behaved similarly to those from TREK-1 in both cell-attached ($\tau = 24.2 \pm 1.5$ ms at −50 mmHg; $n = 16$) and after excision ($\tau = 27.1 \pm 1.5$ ms at −50 mmHg; $n = 26$), although the kinetics of desensitization were significantly faster than those of TREK-1 (Fig. 2*A*). The average $P_{1/2}$ value determined by fitting pressure-effect curves with a Boltzmann function (see Fig. 6*D*) was −65.0 ± 3.4 mm Hg (significantly different from TREK-1; $P < 0.01$) and the slope factor k was 8.1 ± 0.5 ($n = 15$). Similar transient currents were elicited by positive pressure pulses applied to inside-out patches, although these were usually of smaller amplitude than currents recorded at negative pressure (see ref. 14 and Fig. 2*B*). A striking feature of the kinetics is that the channels closed immediately when the pressure returned to zero (Fig. 2*C*). Recovery from desensitization required ≈1 s (Fig. 2*D*).

The data discussed were mean currents from multichannel patches. Is it possible that desensitization involves time-dependent occupancy in subconductance states, as has been reported for cationic mechanosensitive channels (26)? Single channel recordings at low expression density showed desensitization, but no obvious change in unitary conductance with time; desensitization appeared as a reduction in the opening rate with time (Fig. 2*E*).

In contrast to TREK-1 and TRAAK, TREK-2 showed a high level of basal current and little or no desensitization in cell-attached or inside-out configurations (Fig. 3 *B*, *D*, and *E*). This observation supports the idea that desensitization does not arise from the cytoskeleton, because that is expected to be similar after transfection with different channels [although see our previous report showing that cytoskeleton structure can be coupled to specific K_{2P} channel expression (25)]. The average $P_{1/2}$ value determined by fitting pressure-effect curves with a Boltzmann function (see Fig. 6*D*) was −49.9 ± 5.0 mmHg and $k = 18.3 \pm 1.3$ (significantly different from TREK-1; $P < 0.001$; $n = 22$).

The large basal current of TREK-2 exposes some interesting kinetic features. Although the onset of currents appeared monotonic, in detail there was an initial transient inhibition (Fig. 3 *B* and *D*) and a larger transient inhibition when the stimulus was removed (Fig. 3 *B*, *D*, and *E*). This effect is because of complex

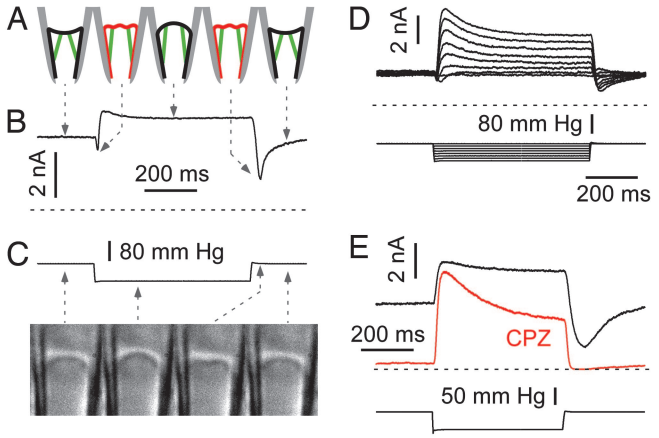

Fig. 3. Desensitization of TREK-2. (*A*) Cartoon illustrating patch mechanics at different times during a suction pulse protocol. The patch is shown concave at rest from normal forces from the cytoskeleton (35). (*B*) Currents at high time resolution from a cell-attached patch showing the effect of membrane stretch, wrinkling, and reannealing of the seal. Holding potential was 0 mV at physiological K^+ gradient. Pulses were applied every 3 s (lower trace). (*C*) Time sequential images (left to right) of a patch from a mouse myotube showing the patch at rest, stretching under suction, wrinkling, and then reannealing upon return to zero pressure. Leftmost image (0 ms), the resting membrane (convex in this case) at zero pressure; second image from left (450 m after application of a −50 mmHg pressure step), when the patch bulges upward; third image from left (50 ms after the return to zero pressure), the patch wrinkles because there is excess area; and rightmost image (1 s after return to zero pressure), the patch returns to rest by reannealing to the glass. The arrows are indicative of the pressure conditions. (*D*) TREK-2 has minimal desensitization in the inside-out configuration. Notice the wrinkle effect at onset and offset of the pulses. Holding potential was 0 mV in physiological K^+ gradient with pressure pulses every 3 s. (*E*) Chlorpromazine (CPZ; 50 μM) applied intracellularly shifts the midpoint of the gating curve to higher pressures, reduces resting current, and speeds up desensitization. Notice that the ''tail current'' due to wrinkling is exceptionally large because of the large resting current. This tail current is inhibited by CPZ. Holding potential was 0 mV, with pressure pulses every 3 s in physiological K^+ gradient. Zero current is indicated by the dashed lines.

patch mechanics (Fig. 3 *A* and *C*). In a resting patch, adhesion of the patch to the glass (the seal) creates a resting tension of several millinewtons per meter (27, 28). The patch with zero applied pressure, is usually orthogonal to the glass (26, 29) but may be bowed in either direction by normal stresses from the cytoskeleton (Fig. 3*A*). The TREK-2 channels and TREK-1 treated with pH or amphipaths were active at zero pressure because the seal adhesion energy produces tension (Fig. 3 *B*, *D*, and *E*). The resting tension also can be increased by cytoskeletal forces bowing the patch. The membrane area to span the pipette as a disk at radius r is πr^2 and is less than the area of the spherical cap, $2\pi rh$, where h is the height of the cap, if the unstimulated patch were bowed toward the tip. Thus, suction would initially move the patch to a position approximately normal to the pipette walls, and because there is now excess area, the patch will buckle, relieve the resting tension (Fig. 3*A*), and turn off the channels. This effect accounts for the initial transient reduction in current (Fig. 3 *B* and *D*). A similar, but larger, effect follows the termination of the stimulus (Fig. 3 *B*, *D*, and *E*). The reduced tension due to buckling was restored over a period of ≈500 ms by the membrane reannealing to the glass (Fig. 3 *A*–*E*). Buckling of the patch increases the local curvature in both directions, but always leads to channel closing. Thus, membrane curvature, *per se*, cannot account for channel activation, and we favor the traditional interpretation that the primary stimulus for activation is tension, not curvature. This stretch-inactivated responses we observed suggests that ''stretch-inactivated channel'' activity (30) may actually arise from stretch-activated channels recorded under mechanical prestress.

However, channel activity may be modulated by local curvature or monolayer expansion as suggested by the asymmetric effects of amphipaths (see below and refs. 13 and 16). For example, the high resting activity of TREK-2 was inhibited by application of the cationic amphipath chlorpromazine (CPZ) (Fig. 3*E*). Interestingly, CPZ ($n = 4$) increased the rate of desensitization (Fig. 3*E*), as would be expected if it was acting in the same mode as decreased pressure. The amphipaths prestress the channels, changing the preexponential factors in the rate constants (see below).

The primary features of the data can be summarized in a simple kinetic model that accounts for the following: (*i*) the current develops with a latency; (*ii*) the peak current monotonically tracks the stimulus, although the time to peak is nearly independent of the magnitude (see Fig. 7*A*, which is published as supporting information on the PNAS web site); (*iii*) desensitization slows as channels reach saturation (Fig. 7 *A* and *B*); and (*iv*) the off response is nearly instantaneous; i.e., the channels can respond rapidly to changes in applied stress, suggesting that the local stresses are not significantly delayed in the conversion of pressure to tension (Fig. 2*C*). These features require a minimum of four states, and the simplest topology is linear (see Fig. 8 *A* and *B*, which is published as supporting information on the PNAS web site). The model has seven adjustable parameters: the number of active channels in the patch, the three reverse rate constants (assumed to all be equal and independent of pressure), and the three forward rates, two of which are pressure dependent (Fig. 8*B*). Suction increases the activation rate k_{23} and slows the desensitization rate k_{34}.

To simplify the following discussion, the convention for rate constants within QUB (www.qub.buffalo.edu) is: $k_{ij} = k_{ij}^0 \exp(k_{ij}^1 \cdot P)$, where k_{ij}^0 is the stimulus-independent part of the rate constant, and k_{ij}^1 is the stimulus sensitivity, in units of the inverse stimulus, P. Although the actual stimulus is local stress and not the applied pressure (23), for convenience we will refer to the stimulus as pressure. k_{ij}^1 is the pressure required to obtain an e-fold increase in the rate, with the convention that a negative value refers to a rate that speeds up with suction. Because tension is an even function of the pressure gradient, this formulation of the rates cannot be used for stimuli containing both positive and negative pressures. The fit of data to the linear model of Fig. 8*A* is reasonable, although not precise. The deviations are more systematic than random, hence it is not possible to compare models by using probabilistic standards such as likelihood, and furthermore, precision modeling is inappropriate because the local stimulus is not reliably known (cf. Fig. 3). The model has asymmetric pressure-sensitive rates (Fig. 8*B*) as shown for MscL (31), suggesting that the transition state is located close to the open state. This result is expected if the closed channel is more compliant than the open channel.

The stimulus dependence of the opening rate for the data of Fig. 8*A* is $k_{23}^1 = -0.06$/mmHg and varies between patches from −0.03 to −0.10. To turn this number into a physically meaningful value, we will estimate the tension T in the membrane and calculate the work done going between closed and open as $\Delta G = T\Delta A$, where ΔA is the difference of in-plane area (23, 24, 31). By formulation of the rate constants, $\Delta G/k_BT = P \cdot k_{23}^1$, where P is the pressure and $k_BT = 4.1$ pN·nm. From Laplace's law, $T = Pr/2$, where r is the radius of curvature of the patch. Solving, $\Delta A = 2k_BT \cdot k_{23}^1/r$. The minimum value of r is the radius of the pipette (27, 29) and provides the maximum estimate of ΔA. Assuming $r > 1$ μm and converting k_{23}^1 to Pa, $\Delta A > 1.8$ nm^2. This value can be compared with the mechanosensitive bacterial channel, MscL, where $\Delta A \sim 20$ nm^2 (31, 32). If the channel is approximated as a cylinder 5 nm in diameter, the change of radius accounting for $\Delta A = 0.1$ nm, a remarkably

BIOPHYSICS

small change, probably accounting for the ease by which amphipaths alter the rates.

The pressure sensitivity of the desensitization rate (Fig. 8*B*; $k^1_{34} = 0.06$/mmHg) reflects an equal decrease in channel area, so that the dimensions of the desensitized state would be about the same size as the resting state. The numeric values apply, in detail, only to this data set. Systematic errors such as tension being shared between the bilayer and the cytoskeleton (27) and the presence of resting tension so that zero pressure is not zero stimulus will cause underestimates of ΔA and Δr. The preexponential factor of the rate constants is the rate at zero pressure and as shown above relates to the midpoint of the Boltzmann distribution.

Can we use kinetic modeling to judge whether desensitization is a property of the channel itself (inactivation) (2, 33) or represents relaxation of the stimulus, i.e., adaptation (5)? The simplest test would be to open all of the channels, let them desensitize, and then increase the stimulus further to see whether they can still open. If the channels are inactivated, for example, by plugging the pore, then they cannot reopen with the increased stimulus. On the other hand, if the stimulus has locally adapted, the channels can be reopened. The results of such an experiment are shown in Fig. 8*C*, modeled with the linear four-state model. The reasonable fit to a model without adaptation shows that, in general, this protocol is not a good test of adaptation. Because the rates are exponential in the stimulus, the increased stimulus of the second pulse can easily produce additional current if the channels are not fully saturated. In our case, the rate of desensitization was too rapid to permit saturation without breaking the patch.

Although the linear model fits the main kinetic features of a response to simple stimuli (Fig. 8*A*), it proved inadequate to fit more complex stimuli (Fig. 4). For example, in the classic protocol to measure the time course of recovery from inactivation (Fig. 4*D*), the linear model will not restore channels to the resting state sufficiently rapidly to have them reopen at the observed rate. However, by closing the model into a loop (Fig. 4*B*), we could model both the simpler kinetics and the recovery from inactivation (Fig. 4 *A* and *D*). The model used in Fig. 4*D* has 10 constraints on 17 parameters, leaving only 7 independent parameters. Although the apparent desensitization rate (as fit by an exponential to the descending phase of the current) is a function of several rate constants, the cyclic model fits the data, including the slowing of desensitization with pressure (Figs. 4 *A* and *B* and 7 *A* and *B*). The model predicted the observed slowing of desensitization with a conditioning stimulus (Fig. 4*C*) and the response to a ramp, although the fit (Fig. 4*E*) reminds us of the nonideal patch mechanics, especially during stimulus turn-on and turn-off.

Excision commonly causes a rundown of mechanosensitive channels (5, 26, 34), but K_{2P} channels undergo "run up" (Figs. 1 *A* and *B* and 2*A*; see also refs. 14 and 25). The run up results from an increase in the number of available channels rather than a change in the rates. Channels seem to lose their "mechanoprotection" with time, probably reflecting a breakdown of the cytoskeleton exposing the bilayer to a larger fraction of the applied stress (5, 26, 35, 36). The effect of patch excision is actually mimicked by latrunculin A treatment in the cell-attached configuration (see ref. 25 and Fig. 6*B*).

As a test of the possible involvement of the cytoskeleton in desensitization, we recorded activity in blebs of *Xenopus* oocytes (37) (see Fig. 9*B*, which is published as supporting information on the PNAS web site). The blebs have been reported to be deficient in actin and tubulin and devoid of microvilli, so that channel activity may more closely emulate bilayer reconstitution (37). TRAAK currents desensitized in cell-attached mode from normal membrane and blebs (Fig. 9 *B–D*), suggesting that desensitization is a property of the channels themselves.

The assignment of desensitization to the channel predicts that changes in channel structure should affect desensitization. Cytoplasmic acidity activates TREK-1 channels through protonation of Glu-306 in the cytosolic C-terminal domain (20). What is the effect of acidic intracellular pH (pH_i) on desensitization? There was a large increase in the resting current consistent with the midpoint of the gating curve moving to lower stress (Fig. 5*A*; see also ref. 19). E306A emulates acidosis, and the high resting activity creates a pronounced "tail current" when the pressure returned to zero because of buckling of the patch (Fig. 5*B*). As predicted from the kinetic model (Fig. 4*B*), speeding up the pressure-dependent rates by using the preexponential factors leads to a significant loss of desensitization (Fig. 5 *A* and *B*; see also Fig. 10*A*, which is published as supporting information on the PNAS web site).

The C-terminal domain of TREK-1 plays a key role in regulating channel function (19–21). When the last 100 aa of this domain were deleted, the sensitivity to stretch was dramatically decreased; i.e., the pressure–effect curve was shifted to the right without apparent alteration of the slope (see refs. 13 and 19). Desensitization became significantly faster ($\tau = 22.4 \pm 3.1$ ms at -50 mmHg; $n = 20$) as compared with TREK-1 WT ($\tau = 46 \pm 4.2$ ms at -50 mmHg; $n = 28$, Figs. 5*C* and 10 *A* and *B*). A decrease in pH_i, increased the current of ΔC100 by shifting $P_{1/2}$ toward lower pressures, but the currents remained transient (although slower; Fig. 10*B*), showing that that the last 100 aa

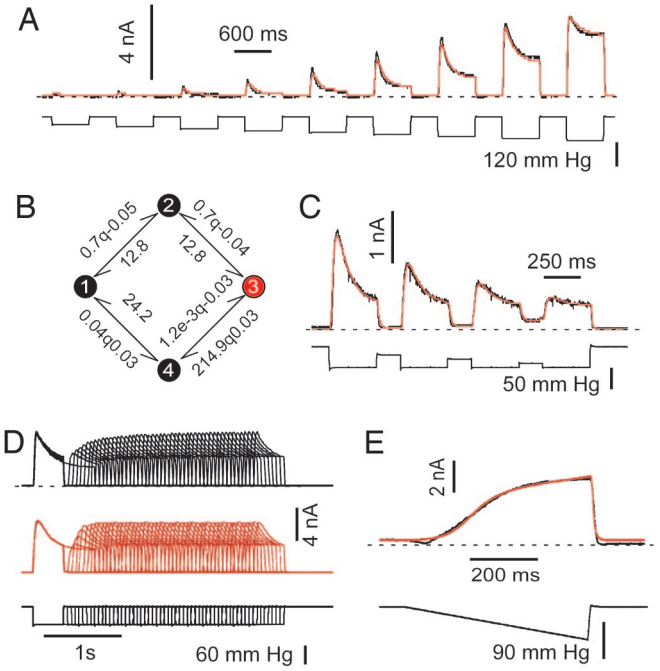

Fig. 4. Four-state cyclic kinetic model accounting for the pressure dependence and the recovery from desensitization of TREK-1 and TRAAK. (*A*) Pressure dependence of desensitization for a TREK-1 inside-out patch. The top black trace is the data, and the red trace is the global fit to that data. The pressure stimulus is shown in the lower black trace. Holding potential was 0 mV in physiological K^+ gradient (see Fig. 7). Shown is a series of nine test pulses depicted end-to-end but actually delivered with 3 s between pulses. (*B*) The kinetic model used to fit the data illustrated in *A* (same conventions). The preexponential constants and the pressure sensitivities of k_{12} and k_{23} were arbitrarily constrained to be equal, as were the rates k_{34} and k_{41}, and k_{32} and k_{21}. (*C*) TRAAK channel currents in an inside-out patch with a global fit (in red) to the data set by using a model similar to *B*. (*D*) Global fit to data from 50 sets of dual pulse stimuli designed to measure the kinetics of recovery from desensitization. The model contains only seven independent parameters and is in detailed balance at all values of the stimulus. TRAAK channels from an inside-out patch were at a holding potential of 0 mV in physiological K^+ gradient. (*E*) Fit of the same cyclic model to ramp stimulation of an inside-out patch expressing TRAAK. The systematic deviation at the onset of the ramp and the recovery is the result of wrinkling (see Fig. 3).

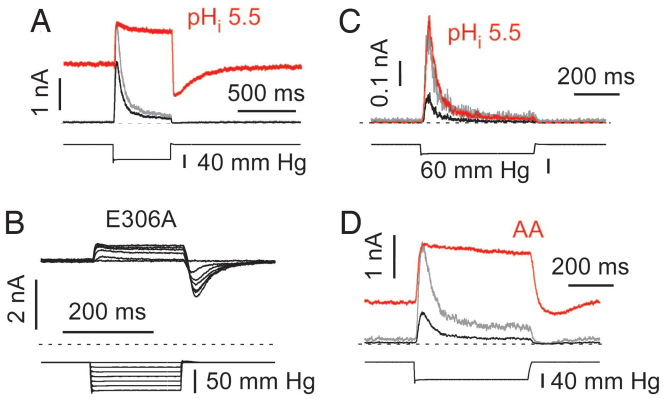

Fig. 5. Prestress removes TREK-1 inactivation. (*A*) At acidic pH$_i$, most desensitization is lost, and the pressure sensitivity increases as expected if the midpoint of the gating curve moves to lower pressure [previously reported for steady-state data (19)]. Black trace, pH$_i$ 7.2; and red trace, pH$_i$ 5.5. Inside-out patch, holding potential 0 mV, with pulses every 5 s in physiological K^+ gradient. Note the large resting current and the tail current due to buckling (see Fig. 3). The control trace amplitude has been normalized (gray trace) to the peak current recorded at pH$_i$ 5.5 to emphasize the different kinetics. (*B*) Removing the negative charge of E306 with an alanine substitution (E306A mutant) has the same effects as lowering pH$_i$ with WT channels. Inside-out patch, holding potential of 0 mV with pulses every 5 s in physiological K^+ gradient. (*C*) The last 100 residues of the C-terminal domain are not necessary for desensitization but do affect the pH$_i$ sensitivity. TREK-1 ΔC100 at a holding potential of 0 mV at pH$_i$ 7.2 (black trace) and pH$_i$ 5.5 (red trace) with a physiological K^+ gradient. The control (gray) trace amplitude has been normalized to the peak current recorded at pH$_i$ 5.5. (*D*) Intracellular 5 μM arachidonic acid increases resting currents and removes desensitization as expected for a shift in the midpoint of the gating curve to lower pressures. Conventions were as in *C*.

were not critical to desensitization (Fig. 5*C*). Note that the midpoint of the pressure–effect curve of ΔC100 at pH$_i$ 5.5 was comparable with the midpoint of TREK-1 WT recorded at pH$_i$ 7.2 (19). The double-mutant ΔC100E306A also desensitized (although slower than ΔC100 at pH$_i$ 7.2, but comparable with the WT channel at pH$_i$ 7.2; Figs. 5*A* and 10 *B* and *C*).

AA and other anionic amphipaths are potent activators of the stretch-sensitive K_{2P} channels, translating the "dose–response" curve to lower pressures increasing the resting current (Fig. 5*D* and ref. 13), probably by generating local stress in the boundary lipids (2, 38–41). Similar to acidic pHi (Fig. 5*A*), desensitization of TREK-1 was removed by AA (Fig. 5*D*).

Discussion

Our primary observation is that the mechanosensitive K_{2P} channels TREK-1 and TRAAK desensitize. The origin of desensitization seems to be an inactivated state of the channel accessible primarily from the open state. Although cytoskeleton reorganization or lipid flow (42) has been proposed to account for desensitization (5), those kinetic tests may have had inadequate resolution to support that conclusion. Furthermore, desensitization persists in membrane blebs with greatly reduced cytoskeleton (37), in the presence of cytoskeleton disrupting agents and after patch excision. However, the cytoskeleton may provide mechanoprotection (36), shielding channels from local stress.

The desensitization of K_{2P} channels differs somewhat from the adaptation mechanism described for other mechanosensitive channels. For example, the desensitization of the endogenous channels in *Xenopus* oocytes (5) and in rat astrocytes (2, 26) has a strong voltage-dependency, slowing with depolarization. The astrocyte channel also uses lower conductance substates to desensitize (2, 26).

The huge currents observed with the K_{2P} channels and the ability to sensitize the channels with acidic pH$_i$, etc., exposed kinetic features of the patch mechanics that have broad implications. Confirming earlier measurements, adhesion energy of the seal is significant (2–3 mN/m) and can activate mechanosensitive channels (27, 28). Seal annealing takes on the order of 1 s. This slow relaxation of a distended patch allows it to buckle during pressure transients, creating a minimal stress environment and thus transient reductions in mechanosensitive current.

K_{2P} channels are modulated by various second messengers (for review, see refs. 17 and 43). These effects are well accounted for by translation of the activation curve to lower pressures, as though the channel was chemically prestressed (13, 19). The C-terminal domain of TREK-1 interacts with the plasma membrane, probably by means of electrostatic interactions between a cluster of positive charges (a PIP_2 interacting domain) and anionic phospholipids (21). This interaction is affected by protonation of E306 (20, 21) and may prestress the channels. The distal C-terminal domain, however, is not essential for desensitization.

The differential effects of cationic and anionic amphipaths suggest that the channel is sensitive to asymmetric stresses and perhaps membrane curvature (13). However, we can maintain the physical model using far-field tension for activation if the channel opens asymmetrically with respect to the inner and outer monolayers, i.e., activation involves a torque (23). The small dimensional changes required to explain the mechanical sensitivity, 0.1–0.2 nm, suggest that amphipaths could readily distort the boundary lipids and produce equivalent stress.

The presence of desensitization implies that in the physiological setting, transient stimuli can have large effects without the channels dominating the steady-state background. This hypothesis may explain the "knockout punch," where a blow to the head activates K_{2P} channels, hyperpolarizing neurons, and producing transient unconsciousness. This paradigm fits well with data showing that K_{2P} channels are activated by general anesthetics at clinical doses (7, 44).

TREK-1 may play a key role in neuroprotection against ischemia (7, 17, 18). During brain ischemia, neurons swell, AA is released, and intracellular acidosis occurs, reducing desensitization and activating the channels (for review, see ref. 18). The resulting hyperpolarization decreases Ca^{2+} overload that causes excitotoxicity (18).

TREK-2 channels have recently been described in astrocytes where they are proposed to play a functional role in the regulation of K^+ homeostasis (45) where their mild desensitization thus be physiologically useful for the slower process of K^+-siphoning.

Materials and Methods

COS cell culture, *Xenopus* oocyte handling, channel mutagenesis, transfection, mRNA injection, patch imaging, and the electrophysiological procedures have been detailed elsewhere (13, 19, 25, 26, 29). The patch pipette medium contained 150 mM NaCl, 5 mM KCl, 3 mM $MgCl_2$, 1 mM $CaCl_2$, and 10 mM Hepes (pH 7.4) with NaOH. To study the voltage-dependency of TREK-1, we used a pipette medium containing 155 mM KCl, 5 mM EGTA, 5 mM EDTA, and 10 mM Hepes (pH 7.4) with KOH. The bath medium contained 155 mM KCl, 5 mM EGTA, 3 mM Mg^{2+}, and 10 mM Hepes (pH 7.2) with KOH. In some experiments, intracellular Mg^{2+} was omitted, and 5 mM EDTA was included. For further details, see *Supporting Materials and Methods* and Fig. 11, which are published as supporting information on the PNAS web site.

We thank Pr. Michel Lazdunski for support and stimulating discussions and Martine Jodar for expert technical assistance. E.H. and A.J.P. were supported by the Agence Nationale de la Recherche Cardiovasculaire-Obésité-Diabète. F.S. and T.S. are supported by the National Institutes of Health and the Oshei Foundation.

1. Hamill, O. P. & Martinac, B. (2001) *Physiol. Rev.* **81,** 685–740.
2. Suchyna, T. M., Tape, S. E., Koeppe, R. E., Andersen, O. S., Sachs, F. & Gottlieb, P. A. (2004) *Nature* **430,** 235–240.
3. Blount, P., Sukharev, S. I., Moe, P. C., Martinac, B. & Kung, C. (1999) *Methods Enzymol.* **294,** 458–482.
4. Niu, W. & Sachs, F. (2003) *Prog. Biophys. Mol. Biol.* **82,** 121–135.
5. Hamill, O. P. & McBride, D. W., Jr. (1992) *Proc. Natl. Acad. Sci. USA* **89,** 7462–7466.
6. Fettiplace, R. & Ricci, A. J. (2003) *Curr. Opin. Neurobiol.* **13,** 446–451.
7. Heurteaux, C., Guy, N., Laigle, C., Blondeau, N., Duprat, F., Mazzuca, M., Lang-Lazdunski, L., Widmann, C., Zanzouri, M., Romey, G. & Lazdunski, M. (2004) *EMBO J.* **23,** 2684–2695.
8. Han, J., Truell, J., Gnatenco, C. & Kim, D. (2002) *J. Physiol.* **542,** 431–444.
9. Chemin, J., Patel, A., Duprat, F., Zanzouri, M., Lazdunski, M. & Honoré, E. (2005) *J. Biol. Chem.* **280,** 4415–4421.
10. Koh, S. D., Monaghan, K., Sergeant, G. P., Ro, S., Walker, R. L., Sanders, K. M. & Horowitz, B. (2001) *J. Biol. Chem.* **276,** 44338–44346.
11. Terrenoire, C., Lauritzen, I., Lesage, F., Romey, G. & Lazdunski, M. (2001) *Circ. Res.* **89,** 336–342.
12. Kim, D. (1992) *J. Gen. Physiol.* **100,** 1021–1040.
13. Patel, A. J., Honoré, E., Maingret, F., Lesage, F., Fink, M., Duprat, F. & Lazdunski, M. (1998) *EMBO J.* **17,** 4283–4290.
14. Maingret, F., Fosset, M., Lesage, F., Lazdunski, M. & Honoré, E. (1999) *J. Biol. Chem.* **274,** 1381–1387.
15. Bang, H., Kim, Y. & Kim, D. (2000) *J. Biol. Chem.* **275,** 17412–17419.
16. Lesage, F., Terrenoire, C., Romey, G. & Lazdunski, M. (2000) *J. Biol. Chem.* **275,** 28398–28405.
17. Patel, A. J. & Honoré, E. (2001) *Trends Neurosci.* **24,** 339–346.
18. Franks, N. P. & Honoré, E. (2004) *Trends Pharmacol. Sci.* **25,** 601–608.
19. Maingret, F., Patel, A. J., Lesage, F., Lazdunski, M. & Honoré, E. (1999) *J. Biol. Chem.* **274,** 26691–26696.
20. Honoré, E., Maingret, F., Lazdunski, M. & Patel, A. J. (2002) *EMBO J.* **21,** 2968–2976.
21. Chemin, J., Patel, A. J., Duprat, F., Lauritzen, I., Lazdunski, M. & Honoré, E. (2005) *EMBO J.* **24,** 44–53.
22. Besch, S. R., Suchyna, T. & Sachs, F. (2002) *Pflügers Arch. Eur. J. Physiol.* **445,** 161–166.
23. Markin, V. S. & Sachs, F. (2004) *Phys. Biol.* **1,** 110–124.
24. Wiggins, P. & Phillips, R. (2004) *Proc. Natl. Acad. Sci. USA* **101,** 4071–4076.
25. Lauritzen, I., Chemin, J., Honoré, E., Jodar, M., Guy, N., Lazdunski, M. & Jane Patel, A. (2005) *EMBO Rep.* **6,** 642–648.
26. Suchyna, T. & Sachs, F. (2004) *Phys. Biol.* **1,** 1–18.
27. Akinlaja, J. & Sachs, F. (1998) *Biophys. J.* **75,** 247–254.
28. Opsahl, L. R. & Webb, W. W. (1994) *Biophys. J.* **66,** 75–79.
29. Sokabe, M., Sachs, F. & Jing, Z. (1991) *Biophys. J.* **59,** 722–728.
30. Franco-Obregon, A. & Lansman, J. B. (2002) *J. Physiol.* **539,** 391–407.
31. Sukharev, S., Sigurdson, W., Kung, C. & Sachs, F. (1999) *J. Gen. Physiol.* **113,** 525–539.
32. Chiang, C. S., Anishkin, A. & Sukharev, S. (2004) *Biophys. J.* **86,** 2846–2861.
33. Hille, B. (2001) *Ion Channels of Excitable Membranes* (Sinauer, Sunderland, MA).
34. Bowman, C. L., Ding, J. P., Sachs, F. & Sokabe, M. (1992) *Brain Res.* **584,** 272–286.
35. Sokabe, M. & Sachs, F. (1990) *J. Cell Biol.* **111,** 599–606.
36. Morris, C. E. (2001) *Cell. Mol. Biol. Lett.* **6,** 222–223.
37. Zhang, Y., Gao, F., Popov, V. L., Wen, J. W. & Hamill, O. P. (2000) *J. Physiol. (London)* **523,** 117–130.
38. Perozo, E., Kloda, A., Cortes, D. M. & Martinac, B. (2002) *Nat. Struct. Biol.* **9,** 696–703.
39. Perozo, E., Cortes, D. M., Sompornpisut, P., Kloda, A. & Martinac, B. (2002) *Nature* **418,** 942–948.
40. Perozo, E. & Rees, D. C. (2003) *Curr. Opin. Struct. Biol.* **13,** 432–442.
41. Martinac, B., Adler, J. & Kung, C. (1990) *Nature* **348,** 261–263.
42. Mukhin, S. & Baoukina, S. (2004) *Biol. Membr.* **21,** 506–517.
43. Patel, A. J., Lazdunski, M. & Honoré, E. (2001) *Curr. Opin. Cell Biol.* **13,** 422–428.
44. Patel, A. J., Honoré, E., Lesage, F., Fink, M., Romey, G. & Lazdunski, M. (1999) *Nat. Neurosci.* **2,** 422–426.
45. Gnatenco, C., Han, J., Snyder, A. K. & Kim, D. (2002) *Brain Res.* **931,** 56–67.